Received: 13 June 2024 | Revised: 6 August 2024 | Accepted: 8 August 2024

DOI: 10.1002/alz.14230

Alzheimer's & Dementia®
THE JOURNAL OF THE ALZHEIMER'S ASSOCIATION

RESEARCH ARTICLE

Plasma miRNAs across the Alzheimer's disease continuum: Relationship to central biomarkers

Shiwei Liu[1,2] | Tamina Park[1,2] | Dennis M. Krüger[3,4] | Tonatiuh Pena-Centeno[3,4] | Susanne Burkhardt[3] | Anna-Lena Schutz[5] | Yen-Ning Huang[1,2] | Thea Rosewood[1,2] | Soumilee Chaudhuri[1,2] | MinYoung Cho[1,2] | Shannon L. Risacher[1,2] | Yang Wan[6] | Leslie M. Shaw[6] | Farahnaz Sananbenesi[5] | Alexander S. Brodsky[7] | Honghuang Lin[8] | Andre Krunic[9] | Jan Krzysztof Blusztajn[9] | Andrew J. Saykin[1,2] | Ivana Delalle[9] | Andre Fischer[3,10,11,12] | Kwangsik Nho[1,2,13] | for the Alzheimer's Disease Neuroimaging Initiative

Correspondence
Kwangsik Nho, Department of Radiology and Imaging Sciences, Indiana University School of Medicine, 355 W 16th, GH 4101, Indianapolis, IN 46202, USA.
Email: knho@iu.edu

Andre Fischer, Department for Epigenetics and Systems Medicine in Neurodegenerative Diseases, German Center for Neurodegenerative Diseases (DZNE), Von-Siebold-Str. 3a, Göttingen, 37075, Germany.
Email: a.fischer@mail.gwdg.de

Abstract

INTRODUCTION: MicroRNAs (miRNAs) play important roles in gene expression regulation and Alzheimer's disease (AD) pathogenesis.

METHODS: We investigated the association between baseline plasma miRNAs and central AD biomarkers from the Alzheimer's Disease Neuroimaging Initiative (ADNI; $N = 803$): amyloid, tau, and neurodegeneration (A/T/N). Differentially expressed miRNAs and their targets were identified, followed by pathway enrichment analysis. Machine learning approaches were applied to investigate the role of miRNAs as blood biomarkers.

RESULTS: We identified nine, two, and eight miRNAs significantly associated with A/T/N positivity, respectively. We identified 271 genes targeted by amyloid-related miRNAs with estrogen signaling receptor–mediated signaling among the enriched pathways. Additionally, 220 genes targeted by neurodegeneration-related miRNAs

Shiwei Liu, Tamina Park, Dennis M. Krüger, and Tonatiuh Pena-Centeno contributed equally to this work.

Data used in preparation of this article were obtained from the Alzheimer's Disease Neuroimaging Initiative (ADNI) database (adni.loni.usc.edu). As such, the investigators within the ADNI contributed to the design and implementation of ADNI and/or provided data but did not participate in analysis or writing of this report. A complete listing of ADNI investigators can be found at: https://adni.loni.usc.edu/wp-content/uploads/how_to_apply/ADNI_Acknowledgement_List.pdf

Funding information: Alzheimer's Disease Neuroimaging Initiative; Department of Defense, Grant/Award Number: W81XWH-12-2-0012; NIH, Grant/Award Numbers: U01 AG024904, R01 LM012535, R03 AG063250, R01 AG19771, P30 AG10133, P30 AG072976, R01 AG057739, R01 LM013463, R01 AG068193, T32 AG071444, U01 AG068057, U01 AG072177, U19 AG074879, RF1AG078299, U19 AG024904, P30 AG010133, R01 AG019771, RF1 AG057768, P30 AG013846, RF1 AG072654, U01AG068221, U01 AG058589, R01DK122503; NIGMS, Grant/Award Numbers: P50GM115318, UL1 TR001108, K01 AG049050, R01 AG061788; Alzheimer's Association; Indiana Clinical and Translational Science Institute; IU Health-IU School of Medicine Strategic Neuroscience Research Initiative; National Institute on Aging; National Institute of Biomedical Imaging and Bioengineering; AbbVie; Alzheimer's Drug Discovery Foundation; Araclon Biotech; BioClinica, Inc.; Biogen; Bristol-Myers Squibb Company; CereSpir, Inc.; Cogstate; Eisai Inc.; Elan Pharmaceuticals, Inc.; Eli Lilly and Company; EuroImmun; F. Hoffmann-La Roche Ltd; Genentech, Inc.; Fujirebio; GE Healthcare; IXICO Ltd.; Janssen Alzheimer Immunotherapy Research & Development, LLC; Johnson & Johnson Pharmaceutical Research & Development LLC; Lumosity; Lundbeck; Merck & Co., Inc.; Meso Scale Diagnostics, LLC; NeuroRx Research; Neurotrack Technologies; Novartis Pharmaceuticals Corporation; Pfizer Inc.; Piramal Imaging; Servier; Takeda Pharmaceutical Company; Transition Therapeutics; Deutsche Forschungsgemeinschaft, Grant/Award Numbers: 1738, SFB1286, GRK2824; German Federal Ministry of Science and Education; ERA-NET Neuron project; The EU Joint Programme- Neurodegenerative Diseases (JPND), Grant/Award Number: EPI-3E; Germany's Excellence Strategy, Grant/Award Number: EXC 2067/1 390729940; GoBIO project miRassay, Grant/Award Number: 16LW0055; German Federal Ministry of 1 Science and Education

Ivana Delalle, Department of Pathology & Laboratory Medicine, Boston University Chobanian & Avedisian School of Medicine, 670 Albany St, Boston, MA, 02118, USA.
Email: idelalle@bu.edu

Andrew J. Saykin, Department of Radiology and Imaging Sciences, Indiana University School of Medicine, 355 W 16th, GH 4101, Indianapolis, IN 46202, USA.
Email: asaykin@iu.edu

Andrew J. Saykin, Ivana Delalle, Andre Fischer, and Kwangsik Nho directed the study.

showed enrichment in pathways including the insulin growth factor 1 pathway. The classification performance of demographic information for A/T/N positivity was increased up to 9% with the inclusion of miRNAs.

DISCUSSION: Plasma miRNAs were associated with central A/T/N biomarkers, highlighting their potential as blood biomarkers.

KEYWORDS

Alzheimer's disease, amyloid, biomarkers, classification, microRNAs, neurodegeneration, plasma, tau

Highlights

- We performed association analysis of microRNAs (miRNAs) with amyloid/tau/neurodegeneration (A/T/N) biomarker positivity.
- We identified dysregulated miRNAs for A/T/N biomarker positivity.
- We identified Alzheimer's disease biomarker-specific/common pathways related to miRNAs.
- miRNAs improved the classification for A/T/N positivity by up to 9%.
- Our study highlights the potential of miRNAs as blood biomarkers.

1 | BACKGROUND

Alzheimer's disease (AD) is a degenerative neurological disorder that frequently presents as dementia in elderly individuals, resulting in a gradual deterioration of cognitive abilities.[1,2] First, AD has three major neuropathological characteristics. Neuritic plaques occur when extracellular amyloid beta (Aβ) from amyloid precursor proteins accumulates.[3,4] Second, intracellular nerve fiber entanglement arises when hyperphosphorylated tau aggregates in the brain.[3,4] Third, neurodegeneration, demonstrated by the degradation of white and gray matter after neuronal death, can be detected by techniques such as magnetic resonance imaging (MRI).[3,4] Previous research has introduced "A/T/N" central biomarkers. "A" indicates the Aβ biomarker (amyloid positron emission tomography [PET] or cerebrospinal fluid [CSF] Aβ42), "T" represents the tau biomarker (CSF phosphorylated tau or tau PET), and "N" encompasses biomarkers of neurodegeneration or neuronal injury ([18F]-fluorodeoxyglucose PET, structural MRI, or CSF total tau).[5] Blood-based biomarkers such as plasma microRNAs (miRNAs) represent a potential substitute for the current AD biomarkers. They offer advantages of cost savings, accessibility, and decreased invasiveness, potentially yielding additional insights into disease onset and progression.[6]

MiRNAs, short non-coding RNAs with 22 or less nucleotides, are expected to influence approximately half of all protein-coding genes through post-transcriptional processes in gene expression.[7,8] MiRNAs play crucial roles in various biological or pathological processes, such as metabolism, proliferation, differentiation, apoptotic cell death, and molecular mechanisms of diseases.[9] Dysregulation of miRNAs can be an indication of altered cellular states in different tissues and is implicated as a contributing factor in various disorders.[10,11] This highlights the important potential of miRNAs in understanding pathogenesis mechanisms, facilitating diagnosis, and guiding therapeutic strategies for human diseases.

Previous studies have revealed the involvement of miRNAs in AD pathology and the progression of AD, often by targeting AD-related genes or signaling pathways.[12] MiRNAs have emerged as significant contributors to AD progression by controlling key proteins such as amyloid precursor protein and beta-secretase, which are involved in Aβ production.[13–15] Additionally, many miRNAs have been implicated in the progression of AD by directly or indirectly modulating the phosphorylation status of tau proteins.[16–19] Moreover, dysregulation of miRNAs has been implicated in microglial hyperactivation, neuroinflammation, and macrophage polarization in the brain, which play central roles in the pathological cascade of AD.[20,21] Despite decades of research, the etiology of AD is not fully understood, posing challenges for early diagnosis and effective treatment. Understanding the role of miRNAs in the molecular mechanisms underlying AD could offer insights into potential diagnostic markers and therapeutic targets.

The expression patterns of miRNAs have been indicated to vary depending on the time and tissue context.[22,23] MiRNA profiling conducted on brain tissue from individuals from the AD cohort revealed altered expression of specific miRNAs in various brain regions affected by AD.[24] MiRNAs exhibit stability in various biological fluids, such as blood, serum, plasma, and CSF, and previous studies have identified dysregulated miRNAs in AD within these fluid types, though with limited sample size.[25–31] The presence of circulating miRNAs underscores the potential as promising biomarker candidates for AD, as they can

be detected using less invasive techniques, providing valuable insights into AD pathology.

Here, we analyzed the dysregulation of plasma miRNA associated with A/T/N central biomarkers in AD. Baseline plasma samples were analyzed for miRNAs from 803 Alzheimer's Disease Neuroimaging Initiative (ADNI) participants. We identified dysregulated miRNAs related to A/T/N central biomarkers and validated the alteration of selected miRNAs using real-time quantitative polymerase chain reaction (RT-qPCR) data from the ADNI cohort. We also identified the target genes from dysregulated miRNAs and generated functional pathway networks to understand the relationship between target gene enriched pathways and biomarkers. Subsequently, we conducted machine learning classification and evaluated the prediction performance using miRNAs.

RESEARCH IN CONTEXT

Systematic review: The authors reviewed the literature using traditional (e.g., PubMed and Google Scholar) sources, as well as meeting abstracts and presentations. Publications about microRNAs (miRNAs) related to Alzheimer's disease (AD) are cited appropriately throughout the article.

Interpretation: We identified differentially expressed plasma miRNAs related to central amyloid/tau/neurodegeneration (A/T/N) biomarkers for AD. We also reported their target genes and relevant pathways. Additionally, we demonstrated that machine learning classifiers exhibited enhanced performance in distinguishing A/T/N positivity after including differentially expressed miRNAs. These results suggest the potential utility of miRNAs as novel and minimally invasive blood biomarkers for AD.

Future directions: We anticipate that our findings will significantly advance the research on miRNAs in AD and expedite the identification of enhanced AD blood biomarkers. Replication studies and longitudinal analyses for the relationship between plasma miRNAs and central AD biomarkers using independent large-scale cohorts are warranted.

2 | METHODS

2.1 | Study participants

Plasma samples and data used in the study were obtained from the ADNI.[32] The initial phase (ADNI-1) was launched in 2003 to test whether serial MRI, PET, other biological markers, and clinical and neuropsychological assessment could be combined to measure the progression of mild cognitive impairment (MCI) and early AD. ADNI-1 has been extended in subsequent phases (ADNI-GO, ADNI-2, ADNI-3, and ADNI-4) for follow-up of existing participants and additional new enrollments. Demographic information, pre-processed Aβ PET scans, MRI scans, CSF biomarkers, neuropsychological test scores, and clinical information are publicly available and were downloaded from the Laboratory of Neuro Imaging (LONI) ADNI data repository. ADNI CSF biomarkers (Aβ1-42, total tau [t-tau)], and phosphorylated tau [p-tau181]) were generated using the validated and highly automated Roche Elecsys electrochemiluminescence immunoassays.[33] T_1-weighted brain MRI scans were acquired using a sagittal 3D magnetization-prepared rapid gradient echo sequence following the ADNI MRI protocol. As detailed in previous studies,[33] FreeSurfer v6, a widely used automated MRI analysis approach, was used to process MRI scans and extract endophenotypes determined by automated segmentation and parcellation. Pre-processed Aβ PET scans (co-registered, averaged, standardized image and voxel size, uniform resolution) were downloaded and intensity-normalized using a whole cerebellum reference region to create standardized uptake value ratio (SUVR) images.[33] We used CSF Aβ1-42 and Aβ PET accumulation as biomarkers of Aβ plaque ("A"), CSF p-tau as a biomarker of fibrillary tau ("T"), and MRI atrophy and CSF t-tau as biomarkers of neurodegeneration ("N").[5] Amyloid positive was defined as individuals with CSF Aβ1-42 levels < 1098 pg/mL[34] or a whole cerebellum-normalized SUVR > 1.08 for [^{18}F] florbetaben PET[35] and 1.11 for [^{18}F] florbetapir PET,[35] tau positive as individuals with CSF p-tau levels > 19.2 pg/mL,[34] and neurodegeneration positive as individuals with CSF t-tau levels > 242 pg/mL[34] or *z* score–transformed hippocampal volume < −1.5, where *z* scores were calculated from cognitively normal amyloid-negative individuals and adjusted for age, sex, and intracranial volume (ICV).[36] Eight hundred three ADNI participants with miRNA sequencing (miRNA-seq) and AD biomarker data based on neuroimaging and CSF endophenotypes were used for analysis. Demographic data for the ADNI participants can be found in Table 1. The apolipoprotein E (*APOE*) ε4 carrier status is determined by whether a participant has the ε4 allele at the *APOE* gene locus. An participant is considered *APOE* ε4 positive if they have at least one ε4 allele, whether it is one or two copies. Written informed consent was obtained from each participant, and all protocols were approved by each participating study and site's institutional review board.

2.2 | miRNA sequencing

In the previous study,[37] data processing and quality control were performed, and we obtained the processed dataset from the previous study for our analysis. This dataset, derived from Illumina small RNA sequencing, underwent thorough processing steps including adapter trimming, read quality assessment, alignment, count generation, and batch effect evaluation. Notably, the findings from the previous study demonstrated minimal variance within and between the 21 batches, indicating a stable miRNA distribution during library preparation irrespective of sequencing depth. As a result, we used this processed dataset comprising 336 miRNAs and 803 samples that passed quality control measures for our analysis.

TABLE 1 Participant characteristics.

		Biomarkers					
		A		T		N	
Parameter	All	Pos	Neg	Pos	Neg	Pos	Neg
N	803	557	246	536	266	524	279
Age (years)	72.22 ± 7.4	73.01 ± 7.27	70.43 ± 7.39	72.98 ± 7.38	70.67 ± 7.21	73 ± 7.52	70.75 ± 6.94
Sex (F:M)	356:447	235:322	121:125	231:305	125:141	232:292	124:155
Education (years)	16.18 ± 2.65	16.10 ± 2.71	16.37 ± 2.5	15.96 ± 2.68	16.62 ± 2.53	16.06 ± 2.67	16.41 ± 2.62
APOE ε4 positivity (%)	48.69%	61.76%	19.11%	59.89%	26.32%	60.11%	27.24%
Race (1:2:3:4:5:6:7)[a]	1:11:2:25:753:10:1	1:5:1:15:525:9:1	0:6:1:10:228:1:0	0:6:1:14:509:6:0	1:5:1:11:243:4:1	0:5:0:12:502:5:0	1:6:2:13:251:5:1
Ethnicity (H:NH:U)[b]	30:771:2	21:534:2	9:237:0	16:518:2	14:252:0	13:509:2	17:262:0
Diagnosis (CN:MCI:AD)	165:489:149	77:342:138	88:147:11	72:329:135	92:160:14	67:319:138	98:170:11

Note: Mean ± standard deviation for Age and Education years.

Abbreviations: A, amyloid; AD, Alzheimer's disease; *APOE*, apolipoprotein E; CN, cognitively normal; MCI, mild cognitive impairment; N, neurodegeneration; T, tau.

[a] 1: American Indian or Alaskan Native; 2: Asian; 3: Native Hawaiian or Other Pacific Islander; 4: Black or African American; 5: White; 6: more than one race; 7: Unknown.

[b] H: Hispanic or Latino; NH: Not Hispanic or Latino; U: Unknown.

2.3 | Differential expression analysis of miRNAs with central A/T/N biomarker positivity

Differential miRNA expression analysis was performed using the DESeq2 R package (version 1.42.1).[38] Participants were grouped based on A/T/N positivity. The analysis used the "poscounts" estimator for size factor estimation, handling miRNAs with zeros by calculating a modified geometric mean from non-zero counts. By using the likelihood ratio test (LRT) to detect differentially expressed miRNAs (DE-miRNAs), the analysis evaluated the significance of change in deviance between a full model with each A/T/N biomarker and a reduced model without it.[38] Batch, sex, age, and *APOE* ε4 carrier status were used as covariates. The *p* values were corrected for multiple testing using the default Benjamini–Hochberg (BH) method. MiRNAs with an adjusted *p* value of < 0.05, baseMean ≥ 10, and the absolute value of $\log_2$ fold change ≥ 0.26, were detected as DE-miRNAs. If the adjusted *p* value for a DE-miRNA is smaller than the smallest floating-point value in R (2.225074e-308), it is displayed as 0 for the adjusted *p* value. Additionally, DESeq2 conducts outlier detection on each sample in each gene, thus the *p* value and adjusted *p* value for these miRNAs are marked as NA.[38] We visualized the expression levels of DE-miRNAs as boxenplots (the combination of a boxplot and a violin plot) in Figure S1 in supporting information and summarized literature reviews on the detected DE-miRNAs in Table S1 in supporting information.

2.4 | Linear regression analysis using RT-qPCR miRNA data for validation

We used qPCR data collected from plasma of 155 participants enrolled in ADNI to validate the dysregulation of DE-miRNAs detected in the previous step. Each miRNA was measured with three replicates, and demographic details are available in Table S2 in supporting information. Two DE-miRNAs related to the A biomarker detected by DESeq2 in the previous step are present in the qPCR dataset, including hsa-miR-145-5p and hsa-miR-190a-5p.

Linear regression was performed for the two miRNAs using their mean expression levels from three replicates by the stats package in R (version 4.3.3). MiRNA expression levels were treated as dependent variables, while the biomarker status (A) served as the independent variable. Covariates, including age, sex, and *APOE* ε4 status, were included in the analysis. *p* values for the independent variable were extracted and corrected for multiple testing across the two miRNAs using the BH method. MiRNAs with adjusted *p* values < 0.05 were considered significant in the qPCR dataset.

2.5 | Target gene prediction of miRNAs

Human target genes of DE-miRNAs were extracted from two popular validated target databases, mirTarBase Release 9.0[39] and Tarbase v9.0.[40] MirTarbase is a valuable repository comprising experimentally validated miRNA-target interactions established through various methodologies including next generation sequencing, microarray, and cross-linking and immunoprecipitation, as well as experiments with strong evidence such as qPCR, reporter assay, and western blot.[39] TarBase also provides a comprehensive collection of experimentally verified miRNA targets, with most interactions validated through experiments like high-throughput sequencing of RNA isolated by crosslinking immunoprecipitation, photoactivatable ribonucleoside-enhanced crosslinking and immunoprecipitation, and cross-linking ligation and sequencing of hybrids.[40] To increase the robustness and the reliability of the results, we chose genes that overlapped between the two validated databases as our final target genes (Figure S2, Table S3-S5 in supporting information).

2.6 | MiRNA-target gene network analysis

The miRNA-target gene network was generated based on the interactions between DE-miRNAs and putative target genes which were identified by mirTarBase and TarBase. To identify the potential interactions among target genes, protein–protein interaction (PPI) was retrieved from the STRING database.[41] PPIs were selected by using only experiments as a source and setting the minimum required interaction score to the highest confidence of 0.9. We also examined the overlap between the target genes depicted in the network and the nominated target genes. More than 900 nominated target genes, as provided by Agora,[42] represent novel therapeutic candidates for AD. These candidates were identified through computational analyses of high-dimensional multi-omics data from human samples. The network was visualized by Cytoscape software (version 3.10.1).[43]

2.7 | Pathway enrichment analysis of miRNA target genes

To perform pathway enrichment analysis, the putative target genes were used to Metascape v3.5.20240101.[44] Metascape integrates over 40 knowledgebases, incorporating 11 databases specifically dedicated to enrichment analysis. After functional enrichment analysis, similar terms were clustered based on the calculation of kappa similarity between all enriched term pairs. Using a similarity score cutoff criterion of > 0.3, the network visualized the top 20 clusters of enriched terms for each A- or N-positive group. All enriched pathways are listed in Tables S6 and S7 in supporting information. The network resulting from the pathway analysis was visualized using Cytoscape software (version 3.10.1).[43]

2.8 | Machine learning classification for A/T/N biomarker positivity

First, we extracted normalized read counts from DESeq2, then added 1 for subsequent $\log_2$ transformation. The function of removebatch-effect from limma R package (version 3.58.1)[45] was used to remove

the effect from batch and *APOE* ε4 status. Following the preprocessing steps, we used STREAMLINE (release beta 0.3.4),[46] an automated machine learning pipeline, to apply classifiers to categorize participants into A/T/N-positive and -negative groups. STREAMLINE can apply diverse modeling algorithms and autotuning parameters to achieve the best performance. Ten algorithms were used in this study, including naive Bayes, logistic regression, elastic net, decision tree, random forest, gradient boosting, support vector machine, artificial neural networks, k-nearest neighbor, and genetic programming. Overall, the analysis pipeline comprised the following steps: (1) preprocessing and feature scaling, (2) evaluation and selection of feature importance, (3) modeling and performance evaluation, (4) post analysis including statistic comparison and visualization. These steps are shown in Figure S3 in supporting information. Specifically, 5-fold cross-validation, stratified partitioning, feature filtering, and feature mean/standard deviation scaling on training data and testing data were used during the analysis. During the evaluation and selection of feature importance step, feature importance scores were calculated via mutual information and MultiSURF.[46] After modeling, top feature importance boxplots for each algorithm (across coefficient of variation partitions) were generated. Finally, receiver operating characteristic area under the curve (ROC-AUC) was used as the metric to evaluate the performance of each algorithm.

3 | RESULTS

3.1 | Participant characteristics

The miRNA dataset analyzed in this study, comprising plasma miRNAs, including a total of 803 ADNI participants, with 557 individuals classified as A+ and 246 as A−, 536 as T+ and 266 as T−, and 524 as N+ and 279 as N− (Table 1). Notably, we observed expected differences in *APOE* ε4 carrier percentage between the biomarker-positive and -negative groups (Table 1). This miRNA dataset was comprehensively analyzed to identify dysregulated miRNAs associated with A/T/N central biomarkers, integrating steps including differential expression analysis, qPCR validation, prediction of target genes, generation of miRNA-target networks, pathway enrichment analysis of target genes, and machine learning classification, as shown in Figure 1.

3.2 | Dysregulated miRNAs associated with central A/T/N biomarker positivity

We investigated miRNA alterations associated with AD pathology by analyzing plasma sequencing data comprising 336 miRNAs from 803 participants. Using the DESeq2 LRT and applying filtering conditions of adjusted p value < 0.05, baseMean ≥ 10, and the absolute value of $\log_2$ fold change ≥ 0.26, we identified significant alterations. Specifically, we detected nine miRNAs associated with the A biomarker, eight with the N biomarker, and two with the T biomarker. Of these, three miRNAs were upregulated for A (hsa-miR-483-3p, hsa-miR-145-5p, and hsa-miR-374a-3p) and N (hsa-miR-1180-3p, hsa-miR-337-5p, and hsa-miR-1224-5p), respectively, while six were downregulated for A (hsa-miR-652-3p, hsa-miR-95-3p, hsa-miR-339-5p, hsa-miR-628-5p, hsa-miR-190a-5p, and hsa-miR-3679-5p), and five were downregulated for N (hsa-miR-1255b-5p, hsa-miR-941, hsa-miR-369-5p, hsa-miR-193b-5p, and hsa-miR-215-5p). The results are detailed in Figure 2 and Table S1. Boxenplots in Figure S1A-T illustrate the expression levels of significant miRNAs between A/T/N-positive and -negative groups. Particularly, hsa-miR-483-3p exhibited the smallest adjusted p value (4.75E-24) and the largest $\log_2$ fold change (0.69), indicating upregulation in the A biomarker-positive group compared to the A biomarker-negative group (Figure 2A). Notably, two miRNAs, hsa-miR-337-5p and hsa-miR-1224-5p, overlapped between the T and N biomarkers (Figure 2B-2D). Additionally, we validated the upregulation of hsa-miR-145-5p in the A-positive group compared to the negative group using RT-qPCR data from ADNI. Linear regression analysis revealed a significant association (adjusted p value = 0.014) between hsa-miR-145-5p and the A biomarker, with a coefficient of 0.027 (see the boxenplot in Figure S1U).

We compared the $\log_2$ fold change and adjusted p values of significant miRNAs across A/T/N biomarkers. As previously mentioned, both hsa-miR-337-5p and hsa-miR-1224-5p display significant upregulation in the T and N biomarkers, as shown in Figure 3. Furthermore, while hsa-miR-145-5p is detected as a significant miRNA in the A biomarker, hsa-miR-1180-3p is detected as a significant miRNA in the N biomarker. Although hsa-miR-145-5p demonstrates an adjusted p value < 0.05 in the N biomarker, its $\log_2$ fold change does not surpass the significance threshold of 0.26 (Figure 3). Similarly, hsa-miR-1180-3p shows an adjusted p value < 0.001 in the T biomarker, but its $\log_2$ fold change does not surpass the significance threshold of 0.26 (Figure 3). Nevertheless, both miRNAs demonstrate an upregulation trend across all three phenotypes (Figure 3). Both hsa-miR-190a-5p and hsa-miR-95-3p exhibit significant downregulation in the A biomarker−positive group. Additionally, they both demonstrate an adjusted p value < 0.05 in the T biomarker. However, their expression levels indicate an upregulation trend in T (Figure 3). Both hsa-miR-369-5p and hsa-miR-1255b-5p show significant downregulation in the N biomarker−positive group. Moreover, they both display an adjusted p value < 0.05 in the T biomarker. Consistent with the dysregulation observed in the N biomarker−positive group, their expression levels also suggest a downregulation trend in the T biomarker (Figure 3). Overall, there are more significantly downregulated DE-miRNAs (11) related to A/T/N biomarkers than upregulated DE-miRNAs (6), as shown in Figure 3.

3.3 | Target gene network analysis of significantly dysregulated miRNAs

To elucidate the effect of DE-miRNAs, target genes were identified by intersecting those found in two experimentally validated databases mentioned in the Methods section. Using differential expression results for target prediction, 17 dysregulated miRNAs associated

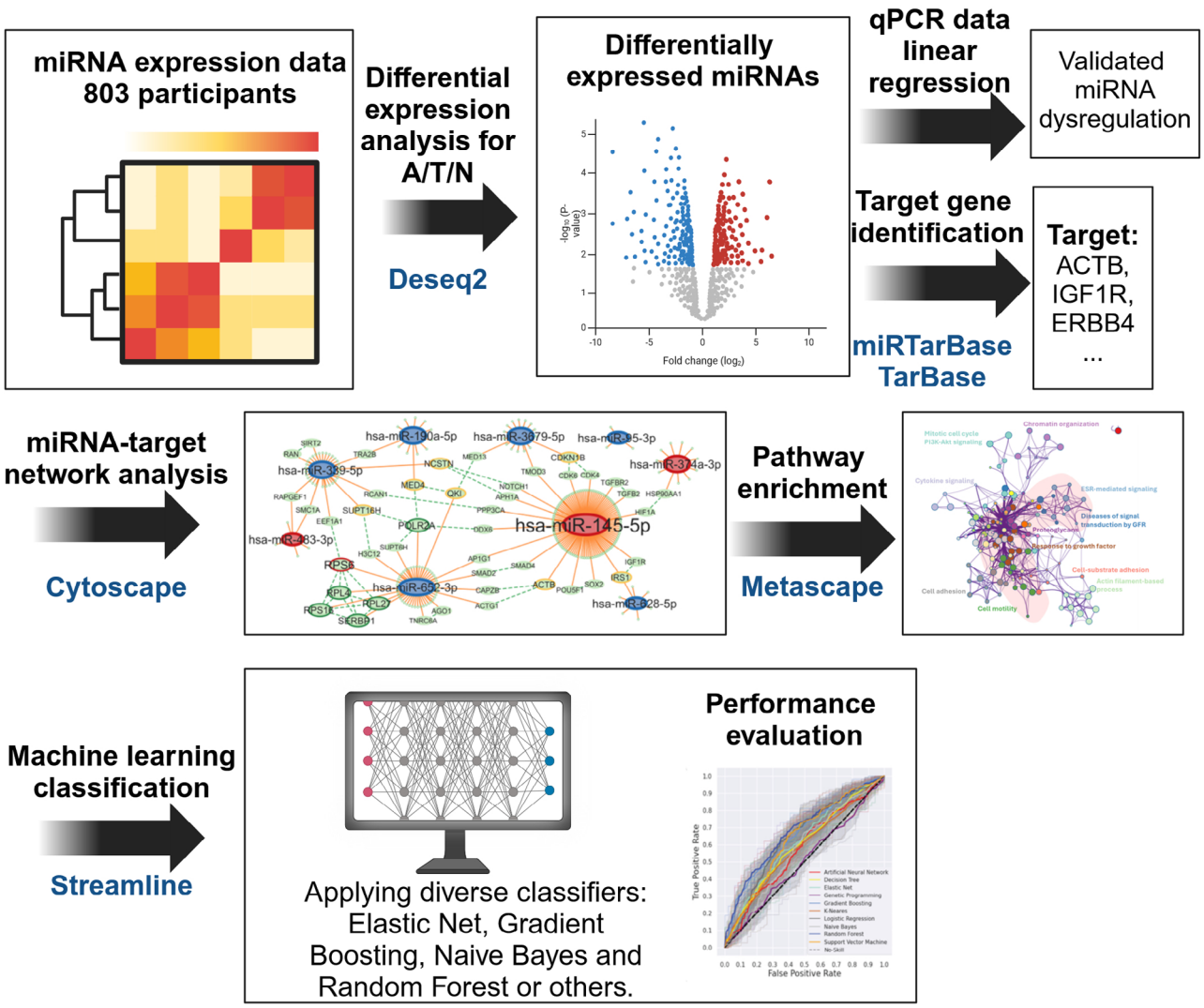

FIGURE 1 Workflow of miRNA-seq analysis with detailed tools and databases. A, amyloid; miRNA-seq, microRNA sequencing; N, neurodegeneration; qPCR, quantitative polymerase chain reaction; T, tau.

with A/T/N positivity were found, resulting in 480 target genes. Two microRNAs (hsa-miR-337-5p and hsa-miR-1224-5p) showed significant expression alteration in both T and N positivity. One target gene was predicted for hsa-miR-337-5p, while nine target genes were found for hsa-miR-1224-5p (Figure S2). All target genes of DE-miRNAs are listed in Tables S3-S5, and the miRNA-target gene network based on their interactions is illustrated in Figure 4.

The miRNA target gene interaction network in the A-positive group showed three upregulated miRNAs and six downregulated miRNAs directly interacting with 271 putative target genes (Figure 4A). *AP1G1*, *TMOD3*, *IRS1*, *RAPGEF1*, *SMC1A*, and *TRA2B* were found to be regulated by two miRNAs. Additionally, *RPS6* exhibited the highest number of interactions with six, followed by *RPL4*, *RPL27*, *RPS16*, and *SERBP1*, all of which interacted with *RPS6* and displayed five interactions, like *POLR2A*. We also compared the target genes having at least two interactions in the network with the nominated target genes in Agora; an overlap was identified, including *QKI*, *IRS1*, *TGFBR2*, *SMAD4*, and *IGF1R*.

In the N-positive group (Figure 4B), three upregulated and five downregulated miRNAs directly interacted with 220 target genes. *CRKL*, *TAOK1*, and *KMT2A* are regulated by two miRNAs. *RPL35* exhibited the highest number of interactions, totaling six. Among the genes interacting with *RPL35*, *RPL19*, *RPL4*, and *EIF5A* displayed five interactions each, while *MRPL9* and *MRPL12* exhibited two interactions. Through a comparison of target genes with at least two interactions in the network with nominated target genes in Agora, we found that the mitochondrial ribosome protein L12 (*MRPL12*) overlaps.

3.4 | Pathway enrichment analysis of target genes of significantly dysregulated miRNAs

The putative target genes were subjected to pathway enrichment analysis to investigate the molecular mechanisms behind miRNA expression alterations in A/T/N positivity. Enrichment analysis of the target genes revealed a variety of pathways (Tables S6 and S7, Figure 5). In

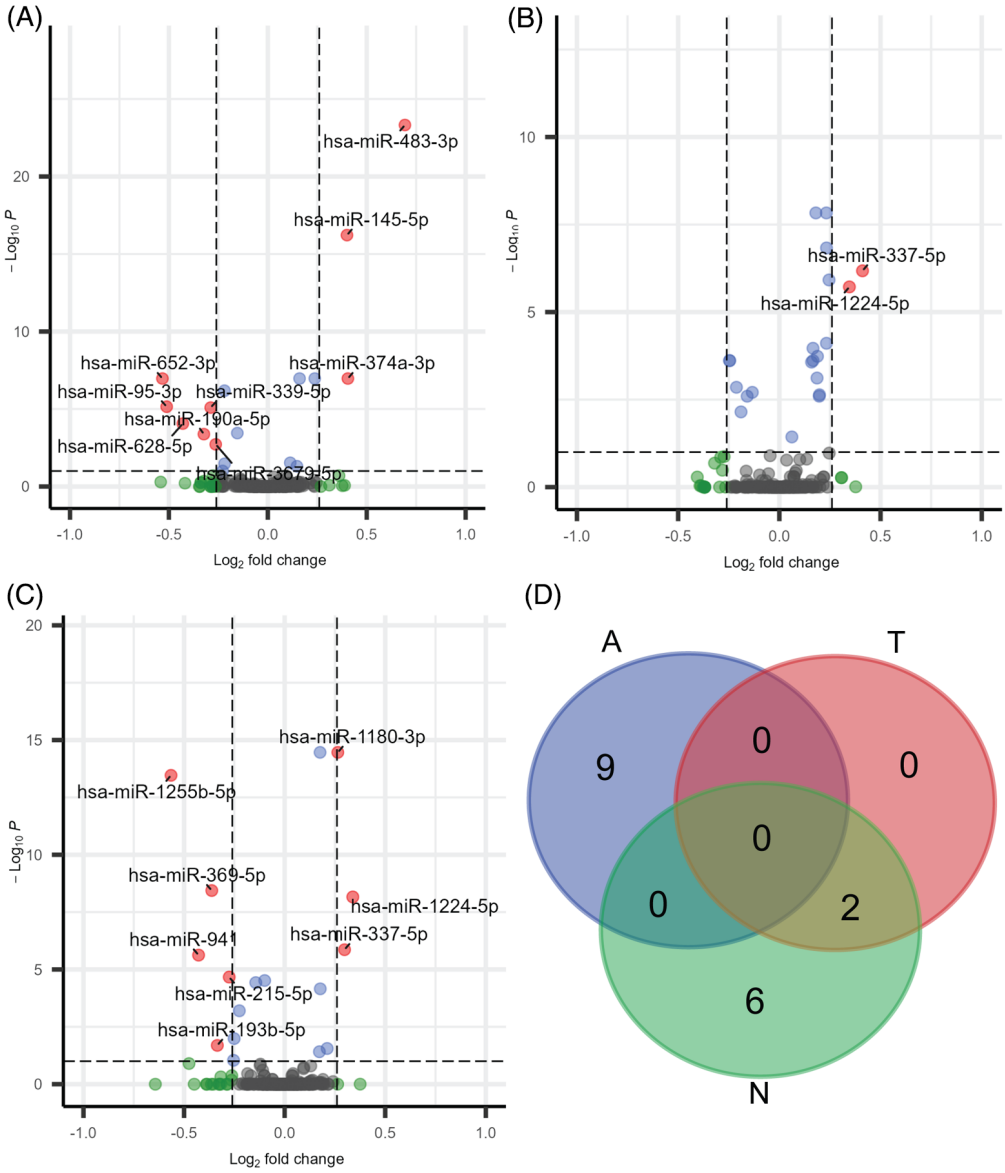

FIGURE 2 Volcano and Venn plots of miRNAs related to the A/T/N biomarkers. A, Volcano plot for miRNAs identified related to the A biomarker. B, Volcano plot for miRNAs identified related to the T biomarker. C, Volcano plot for miRNAs identified related to the N biomarker (hsa-miR-1180-3p has an adjusted *p* value smaller than smallest floating-point value in R, so its adjusted *p* value is displayed as its closest adjusted *p* value listed [3.44E-14]). Note: miRNAs with a baseMean < 10 are not shown in the volcano plot; red colored dots represent miRNAs with an absolute value of $\log_2FC \geq 0.26$ and adjusted *p* value < 0.05; blue colored dots represent miRNAs with an adjusted *p* value < 0.05; green colored dots represent miRNAs with an absolute value of $\log_2FC \geq 0.26$; gray colored dots indicate miRNAs that failed to pass these conditions. D, Venn plots of significant miRNAs detected in the three A/T/N biomarker groups. A, amyloid; $\log_2FC$, $\log_2$ fold change; miRNA-seq, microRNA sequencing; N, neurodegeneration; T, tau.

Figure 5A, the 151 pathways enriched with target genes regulated by miRNAs significantly related to A positivity included vascular endothelial growth factor 2 (VEGFR2) signaling, signal transduction by growth factor receptors, proteoglycans in cancer, cell-substrate adhesion, and actin filament-based process. In Figure 5B, the network showed additional 169 pathways enriched with target genes regulated by miRNAs significantly related to N positivity including the insulin growth factor 1 (IGF1) pathway, the ErbB signaling pathway, positive regulation of cell migration, and nervous system development. Despite the presence of only 11 target genes common to both the A and N positive group, 28 pathway terms were shared in the network under both conditions (Figure S2 and Figure 5B). The common pathways were divided into several clusters (Table S8 in supporting information). One cluster focused on cell motility-related pathways, including positive regulation of cell migration or locomotion, while another cluster was related to cell projection organization including regulation of neuron projection development. These clusters (GroupID 5 and GroupID 9) were identified in N positivity but merged into one cluster (GroupID 3) in A positivity. Additionally, the related target genes differed between the two clusters, suggesting distinct regulatory mechanisms.

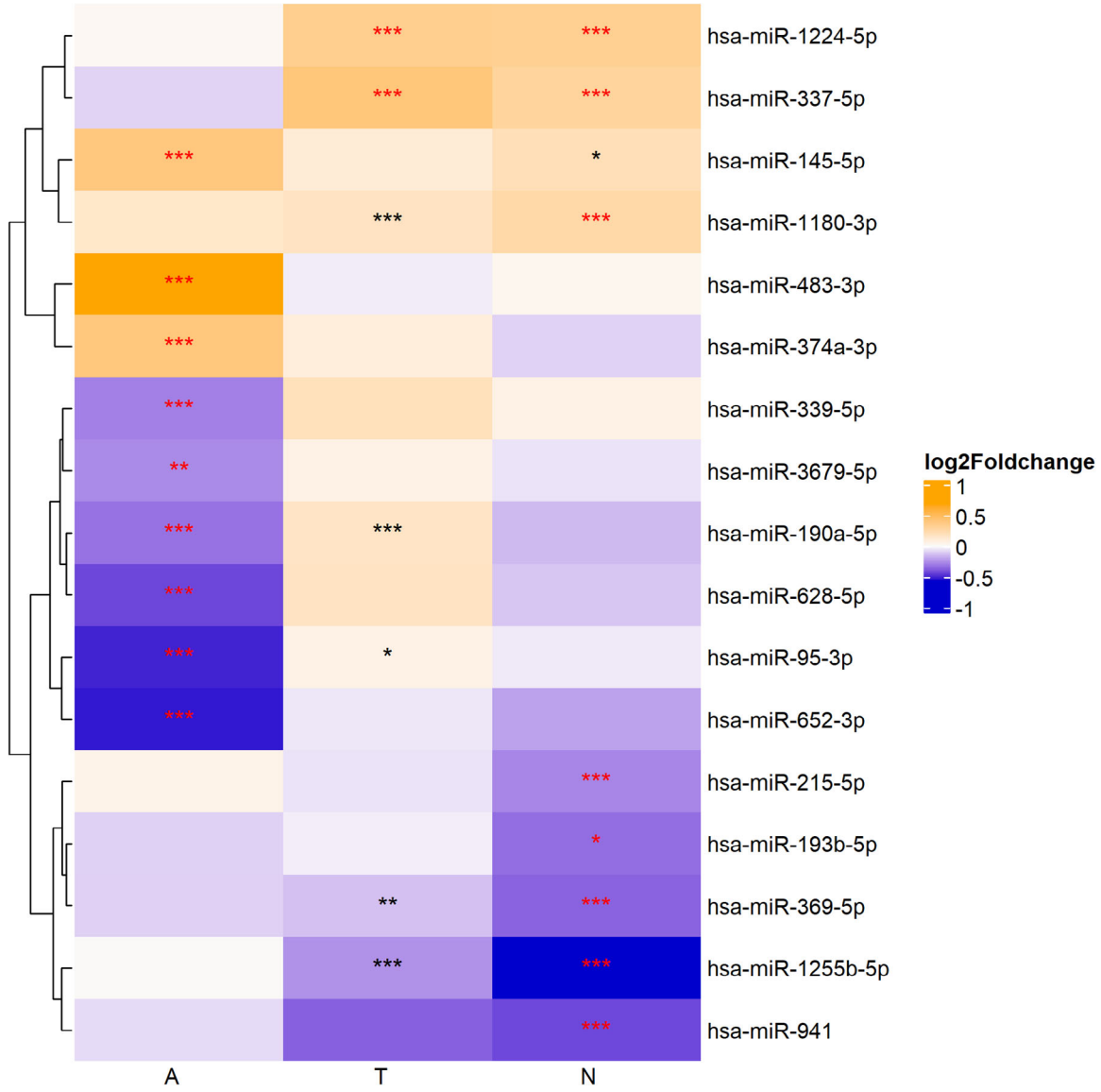

FIGURE 3 Comparison of $\log_2$ fold change and *p* values of significant miRNAs across the A/T/N biomarkers. Note: * indicates 0.01 ≤ adjusted *p* value < 0.05; ** indicates 0.001 ≤ adjusted *p* value < 0.01; *** indicates adjusted *p* value < 0.001. Red stars indicate the absolute value of $\log_2$FC ≥ 0.26 and adjusted *p* value < 0.05. A, amyloid; $\log_2$FC, $\log_2$ fold change; miRNA-seq, microRNA sequencing; N, neurodegeneration; T, tau.

3.5 | MiRNA-driven classification of A/T/N biomarker positivity groups

To evaluate the prediction performance using miRNAs, we used STREAMLINE, an automatic machine learning pipeline, to classify participants into A/T/N positive and negative groups (see the Methods section). We extracted normalized read counts from DESeq2 and adjusted for Batch and *APOE ε4* status effects for the classification (see the Methods section). We compared the performance of each A/T/N biomarker-positive and -negative classification among 10 machine learning algorithms (Figure S4 in supporting information). Random forest achieved the highest ROC-AUC (mean ROC-AUC, A: 0.68; T: 0.62; N: 0.64) for classifying participants to biomarker positive and negative groups with a combination of features including age, sex, and all miRNAs (Figure 6A-D).

Initially, we used age and sex features as the base model and then compared the mean ROC-AUC after incorporating miRNAs into the base model, computed across three independent runs of 5-fold cross-validations. For the A biomarker, we observed a 9% improvement for the mean ROC-AUC when including all miRNAs (from 0.59 to 0.68) and an 8% improvement when including DE-miRNAs (from 0.59 to 0.67; Figure 6D). Similarly, for the T biomarker, we observed a 4% improvement for the mean ROC-AUC when including all miRNAs (from 0.58 to 0.62) and a 3% improvement when including DE-miRNAs (from 0.58 to 0.61; Figure 6D). Last, for the N biomarker, we observed a 7% improvement for the mean ROC-AUC when including all miRNAs (from 0.57 to 0.64) and a 4% improvement when including DE-miRNAs (from 0.57 to 0.61; Figure 6D).

To understand the contribution of different miRNAs to the classification of A/T/N positive and negative groups, we computed the feature

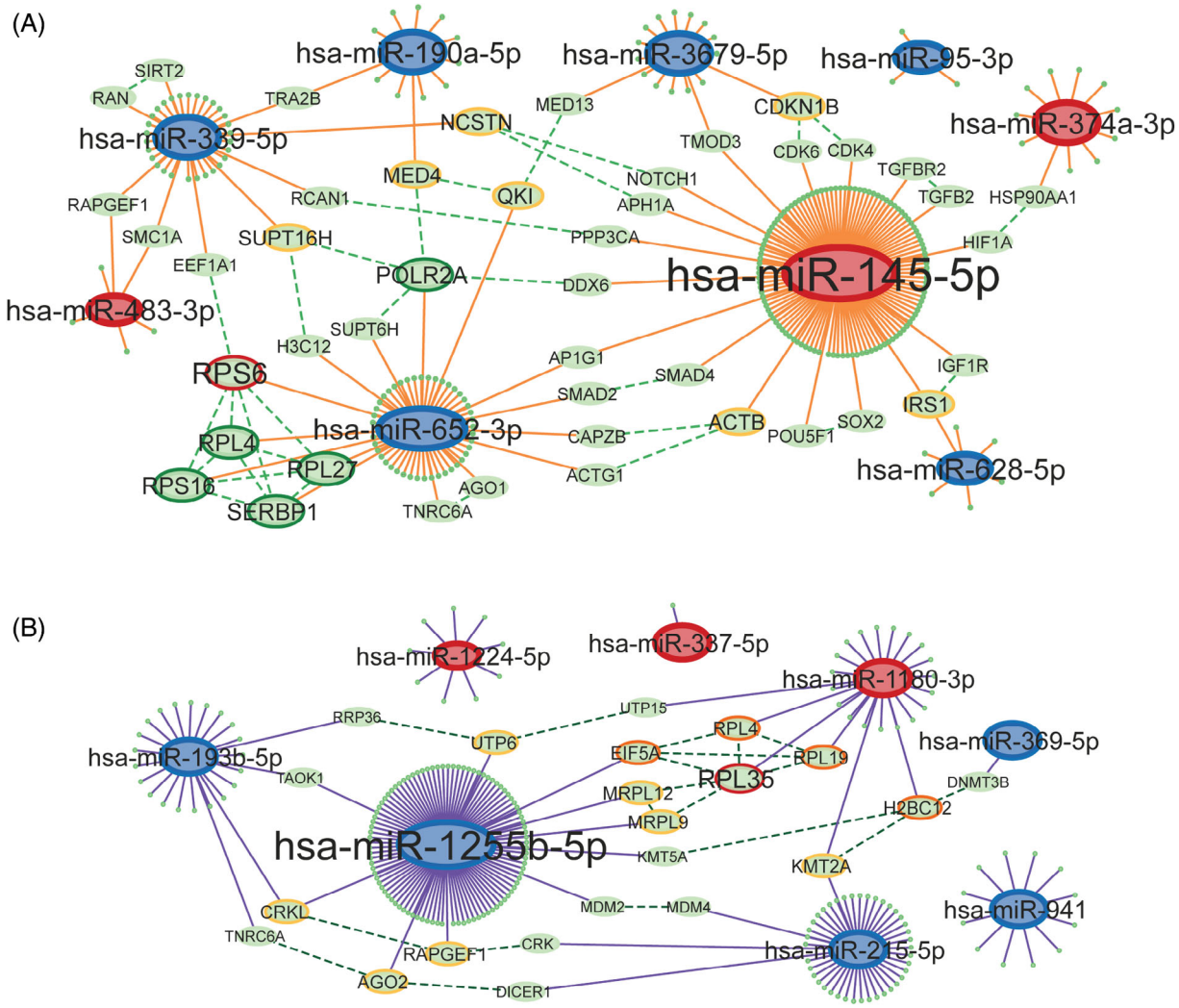

FIGURE 4 MiRNA target gene network. The interaction networks were constructed using target genes of miRNAs significantly associated with either A positivity (A) or N positivity (B). MiRNAs highlighted in red indicate upregulation, while those in blue represent downregulation. The orange or purple solid line denotes miRNA-target interactions predicted by both miRTarBase and TarBase, whereas the green dashed line represents protein–protein interactions sourced from STRING. The border color of target genes corresponds to the number of interactions: yellow for three interactions, orange for four interactions, green for five interactions, and red for six interactions. The network was constructed by the Cytoscape software. miRNA, micro RNA.

importance (FI) scores in STREAMLINE under the random forest model (see the Methods section). The results, as shown in Figure S5, when including all miRNAs as input features and Figure S6, when considering only DE-miRNAs, suggest the importance of individual miRNAs in the classification using Random Forest. In Figure S5, we presented the top 40 miRNAs with the highest FI score when including sex, age, and all miRNAs as input features. Age is the feature with the highest importance for both A and N biomarkers (Figure S5 in supporting information). Consistent with results mentioned earlier, hsa-miR-95-3p and hsa-miR-483-3p were detected both as differentially expressed miRNAs related to the A biomarker and ranked as the top 10 features for classifying the A biomarker groups, see Figure 2A and Figure S5A. Similarly, hsa-miR-1255b-5p, hsa-miR-369-5p, and hsa-miR-193b-5p were detected both as differentially expressed miRNAs related to the N biomarker and ranked as the top 40 features for classifying the N biomarker groups, see Figure 2C and Figure S5C. Additionally, Figure S6 in supporting information displays all DE-miRNAs ranked by FI score when including sex, age, and DE-miRNAs as input features.

4 | DISCUSSION

This study presents a comprehensive miRNA sequencing data analysis for detecting miRNA alterations related to A/T/N central biomarkers. We identified 9, 2, and 8 miRNAs (total 17 unique miRNAs) showing significant differential expression related to A, T, and N positivity, respectively, in plasma-derived samples from ADNI (Figure 2). Two DE-miRNAs overlapped for T and N positivity. The overlap of two miRNAs (hsa-miR-337-5p and hsa-miR-1224-5p) could be due to the definitions of them. The T biomarker is based on CSF p-tau, reflecting tau

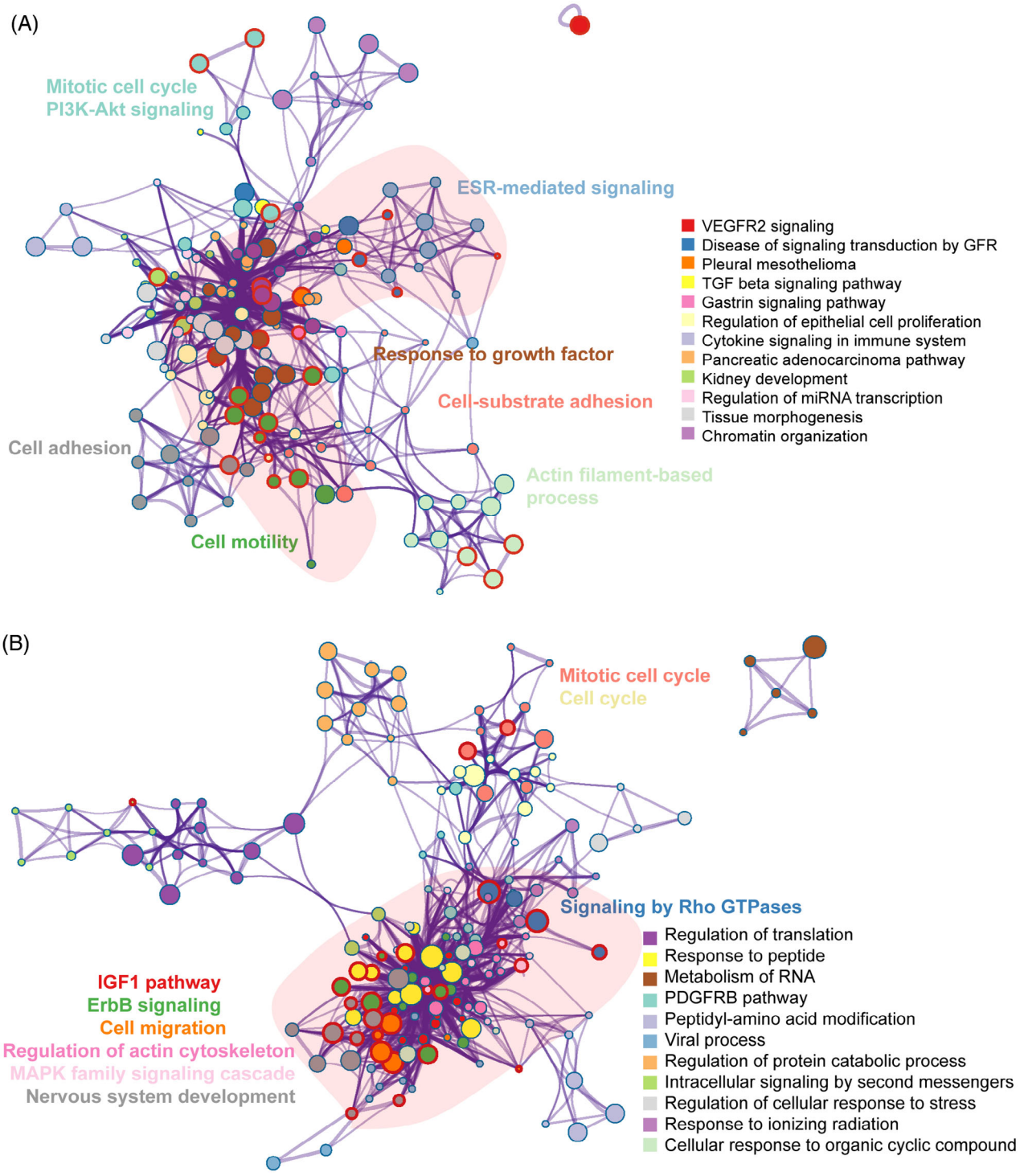

FIGURE 5 Pathway enrichment network. Top 20 clusters of enriched terms in Metascape were generated using target genes predicted by miRNAs significantly associated in A positivity (A) and N positivity (B). The color indicates their cluster ID, while the thickness of the edge reflects the similarity score. The 28 nodes with red borders represent terms that are enriched in both A and N positivity. A, amyloid; N, neurodegeneration.

phosphorylation and tangle formation, while the N biomarker is based on MRI atrophy and CSF t-tau, indicating neuronal damage and degeneration.[5] CSF p-tau and CSF t-tau are often correlated with each other,[47] so the overlap of DE-miRNAs is expected. Moreover, given that tau pathologic burden is known to be linked to the severity of neurodegeneration and clinical symptoms,[48] the overlap of the two miRNAs and their target genes provides further molecular evidence supporting this idea. This finding helps us better understand the molecular mechanisms underlying AD progression and underscores the importance of miRNAs in this process. Overall, there are more

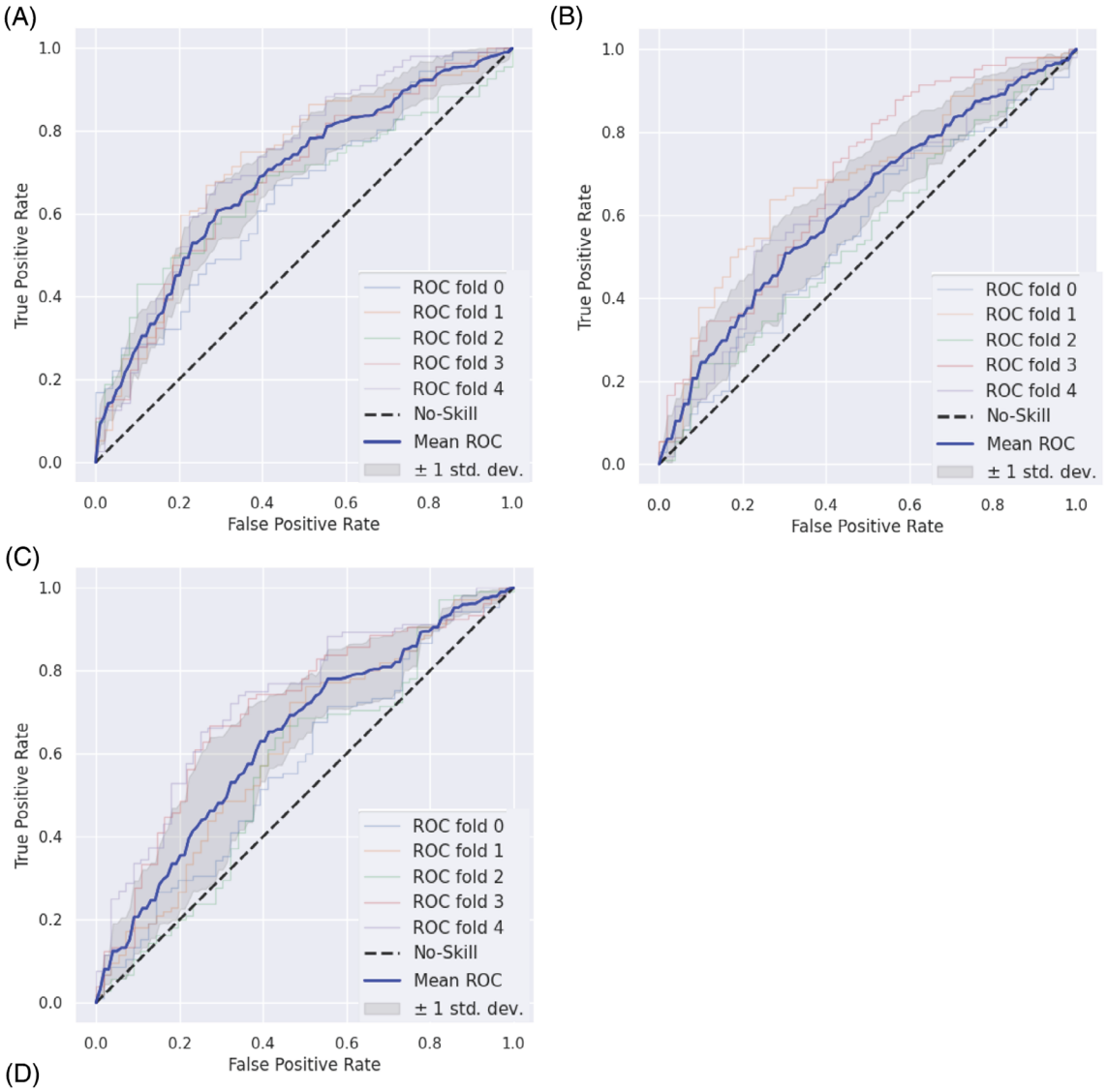

(D)

Biomarkers	Model Features	Balanced Accuracy	Accuracy	F1 Score	Sensitivity (Recall)	Specificity	ROC AUC
A	Age + Sex	0.55±0.03	0.57±0.04	0.65±0.05	0.59±0.08	0.51±0.07	0.59±0.03
	Age + Sex + miRNAs	0.61±0.05	0.67±0.04	0.76±0.05	0.76±0.11	0.45±0.17	0.68±0.03
	Age + Sex + DE miRNAs	0.61±0.03	0.65±0.05	0.73±0.06	0.72±0.11	0.5±0.1	0.67±0.04
T	Age + Sex	0.55±0.03	0.58±0.04	0.66±0.06	0.62±0.1	0.48±0.1	0.58±0.05
	Age + Sex + miRNAs	0.58±0.05	0.62±0.05	0.71±0.05	0.7±0.12	0.45±0.18	0.62±0.05
	Age + Sex + DE miRNAs	0.57±0.04	0.61±0.03	0.7±0.03	0.69±0.06	0.44±0.11	0.61±0.06
N	Age + Sex	0.56±0.03	0.53±0.03	0.55±0.03	0.44±0.04	0.68±0.06	0.57±0.05
	Age + Sex + miRNAs	0.59±0.05	0.63±0.05	0.72±0.06	0.74±0.12	0.44±0.14	0.64±0.07
	Age + Sex + DE miRNAs	0.57±0.03	0.61±0.03	0.69±0.03	0.68±0.05	0.47±0.05	0.61±0.02

FIGURE 6 Classification performance of the A/T/N biomarker positivity using the random forest machine learning algorithm. A, The ROC-AUC curves of classification for amyloid positivity; (B) the ROC-AUC curves of classification for tau positivity; (C) the ROC-AUC curves of classification for neurodegeneration positivity. Note: The dark blue curve indicates the mean AUC curve from 5-fold cross-validation tests and the background curves indicate the ROC curve for each cross-validation fold, while the gray shade indicates the standard deviation of the mean ROC curve; and (D) mean and standard deviation for the performance metrics based on different combinations of features, computed across three independent runs of 5-fold cross-validation. "miRNAs in the Model Features" indicates including all miRNAs in the analysis; "DE miRNAs in the Model Features" indicates including differentially expressed miRNAs for each biomarker in the analysis, respectively. A, amyloid; AUC, area under the curve; miRNA, micro RNA; N, neurodegeneration; ROC, receiver operating characteristic; T, tau.

downregulated DE-miRNAs (11 miRNAs) than upregulated DE-miRNAs (6 miRNAs; Figure 3). Nine novel plasma DE-miRNAs were found to be related to A/T/N in this study after conducting a literature search of known AD DE-miRNAs.

Through a literature search, we found 8 (hsa-miR-1180-3p, hsa-miR-145-5p, hsa-miR-190a-5p, hsa-miR-193b-5p, hsa-miR-339-5p, hsa-miR-369-5p, hsa-miR-483-3p, and hsa-miR-95-3p) of the 17 DE-miRNAs were previously indicated as dysregulated miRNAs in either blood, CSF, or brain tissues in AD.[26–31,49–52] Among the 8 miRNAs, 4 miRNAs (hsa-miR-1180-3p, hsa-miR-145-5p, hsa-miR-339-5p, and hsa-miR-95-3p) show consistent up or down alteration direction as the previous studies, see Table S1. Four miRNAs (hsa-miR-190a-5p, hsa-miR-193b-5p, hsa-miR-369-5p, and hsa-miR-483-3p) show alteration directions conflicting with previous research in blood or CSF (Table S1). This variance may be due to the differences in sample sizes; notably, our study has a much larger sample size, thereby enhancing our confidence in the credibility (see Table S1). Additionally, hsa-miR-193b-5p is known for displaying conflicting alteration directions across blood and CSF samples in AD in previous research.[13,29,30,49] In addition, among the 9 novel DE-miRNAs, 5 (hsa-miR-1225-5p, hsa-miR-1224-5p, hsa-miR-215-5p, hsa-miR-374a-3p, and hsa-miR-628-5p) were known to associate with Parkinson's disease in previous studies,[53–56] suggesting a potential shared molecular signature between AD and Parkinson's disease. Also, hsa-miR-941 is related to brain development in previous studies.[57] For the three remaining novel miRNAs, hsa-miR-652-3p, hsa-miR-337-5p, and hsa-miR-3679-5p are known to be associated with human diseases like cancers.[58–60] Importantly, two plasma DE-miRNAs detected in this study, hsa-miR-145-5p and hsa-miR-339-5p, are previously indicated to be dysregulated in the AD brain (Table S1), underlining their significance in AD and potential as AD biomarkers.

Four hundred eighty target genes were identified for the 17 DE-miRNAs (Figure 4). In the A-positive group, 271 target genes were predicted by three upregulated and six downregulated DE-miRNAs. As shown in Figure 4, RPS6 showed the most PPIs at five, while *RPL4*, *RPL27*, *RPS16*, *SERBP1*, and *POLR2A* followed with four PPIs each. All these target genes were predicted to be directly regulated by hsa-miR-652-3p. In the N-positive group, 220 putative target genes were predicted by three upregulated and five downregulated DE-miRNAs. RPL35 has the highest interactions with five PPIs, followed by *RPL19*, *RPL4*, and *EIF5A* have three PPIs, while *MRPL9* and *MRPL12* have two PPIs. Among these genes, *PRL35*, *RPL4*, and *RPL19* were identified as target genes of hsa-miR-1180-3p, while *MRPL12* and *MRPL9* were predicted as target genes of hsa-miR-1255b-5p. Interestingly, our results revealed interactions in miRNA target networks involving genes related to ribosomal proteins, including *RPL4*, *RPL35*, *RPL19*, *RPL27*, *RPS16*, *MRPL9*, and *MRPL12*. Previous research has demonstrated that disruptions in ribosomal function led to impaired protein synthesis, a reduction in ribosomal RNA and total RNA, and an increase in RNA oxidation in AD.[61,62] Our research highlights that miRNA-target interaction networks, derived from experimentally validated databases, not only corroborate earlier findings[63] but also emphasize the significant role of miRNAs as key regulators of post-transcriptional gene expression.

Pathway analysis with the target genes showed that VEGFR2 signaling, estrogen signaling receptor (ESR)-mediated signaling, and cell-substrate adhesion pathways are enriched for A positivity, and the IGF1 pathway and ErbB signaling pathways are enriched for the N-positive group (Figure 5). Interestingly, VEGFR2 signaling was the most significant pathway in the A-positive group. Additionally, ESR-mediated signaling was exclusively observed in A, while the IGF1 pathway was the most significant in the N-positive group. These differences highlight the unique molecular mechanisms and disease processes associated with each A/T/N central biomarker, providing insights into their distinct roles in disease progression and potential targets for treatment. VEGF is essential for synaptic plasticity, learning, and memory consolidation.[64–67] Previous studies indicate the alteration of VEGF levels is related to AD.[64] The dysfunction of ESR1 has been linked to triggering neuroinflammation.[68] In a recent study investigating the association between IGF1 and cognitive function as well as neuroimaging parameters, the therapeutic potential of IGF1 was highlighted, showing an association with lower white matter hyperintensity volume but not with total brain volume.[69] In our research (Figure 4), *ErbB4* was predicted as the target gene of hsa-miR-145-5p, with significant upregulation in the A-positive group. ErbB4 is known to mediate Aβ-induced neurotoxicity[70] and is involved in various neuronal processes such as neuritic plaques, synapse formation, neuronal migration, and synaptic plasticity through interactions with its ligand NRG1,[71,72] as well as AD pathology.[73]

Eleven target genes were found to be common between A and N, as shown in Figure S2, with some involved in cell motility pathways. A Venn diagram in Figure S2 illustrates the number of overlapped target genes between A and N, revealing the 11 shared genes. Notably, *MDM2*, *RPS6KB1*, *RAPGEF1*, and *ACTG1* are among these genes, suggesting potential shared regulatory mechanisms between A and T. Pathway network analysis further confirmed shared pathways related to cell motility and cell projection organization between the A and T (Table S8 in supporting information). The importance of cell motility in promoting Aβ42 aggregation has been previously demonstrated.[74] However, there are differences between A and N. For instance, although cell motility is a shared pathway between A and N, with 32 target genes in A and 19 in N, only three genes are common to both. This difference in gene count suggests that although the same function is present, it may operate through distinct molecular mechanisms in A and N.

For the machine learning classification, including age and sex as the base model, we observed modest ROC-AUC values of 0.68 for A, 0.62 for T, and 0.64 for N. First, we adjusted the *APOE* ε4 effect in the miRNA data prior to the classification. This adjustment was necessary due to the significantly higher frequency of *APOE* ε4 carriers in the A-positive group compared to the A-negative group, as shown in Table 1. *APOE* ε4 carrier status is known to have a strong effect on A positivity.[75] To address this issue, we adjusted the data by both batch and *APOE* ε4 status prior to the classification. With the modest ROC-AUC values, further research is warranted to identify and validate specific miRNA biomarkers for AD. This could involve exploring combinations of miRNA data with other AD biomarkers to enhance

the accuracy and reliability for predicting A/T/N positive and negative groups.

Several limitations should be considered in our study. First, we observed the zero-inflated count in this miRNA dataset. As shown in Figure S1, many of the detected DE-miRNAs show a high percentage of zero counts, which posed a challenge for the detection of DE-miRNAs. To address this problem, we used the "poscounts" method within DESeq2 for size factor estimation. This method adjusts for genes with zero counts by calculating a modified geometric mean from non-zero counts, thereby mitigating the impact of zero inflation on our analysis. Additionally, we used the LRT to identify DE-miRNAs, evaluating the significance of deviance between a full model incorporating the A/T/N biomarker and a reduced model without it. Through these strategies, we conducted the DE analysis to explore the association between miRNA expression patterns and A/T/N biomarkers. Second, our study solely relied on baseline data, emphasizing the importance of conducting longitudinal analysis in future research. Last, our study used miRNA-Seq data from the ADNI cohort without any replication data. Further studies are warranted to replicate our findings in independent larger cohorts.

The results of this study advance the understanding of miRNA expression and its role in AD. When integrated with other AD biomarkers, these findings may contribute to the development of optimized AD biomarkers, complementing existing blood-based measures. More specifically, these molecular profiles may assist in facilitating early diagnosis and identification of the molecular pathological alterations associated with AD. Continued research on the association between plasma miRNAs and the progression of AD is warranted.

AFFILIATIONS

[1]Center for Neuroimaging, Department of Radiology and Imaging Sciences, Indiana University School of Medicine, Indianapolis, Indiana, USA

[2]Indiana Alzheimer's Disease Research Center, Indiana University School of Medicine, Indianapolis, Indiana, USA

[3]Department for Epigenetics and Systems Medicine in Neurodegenerative Diseases, German Center for Neurodegenerative Diseases (DZNE), Göttingen, Germany

[4]Bioinformatics Unit, German Center for Neurodegenerative Diseases (DZNE), Göttingen, Germany

[5]Research Group for Genome Dynamics in Neurodegenerative Diseases, German Center for Neurodegenerative Diseases (DZNE), Göttingen, Germany

[6]Department of Pathology and Laboratory Medicine, Perelman School of Medicine, University of Pennsylvania, Philadelphia, Pennsylvania, USA

[7]Department of Pathology and Laboratory Medicine, Rhode Island Hospital, Warren Alpert Medical School at Brown University, Providence, Rhode Island, USA

[8]Department of Medicine, UMass Chan Medical School, Worcester, Massachusetts, USA

[9]Department of Pathology & Laboratory Medicine, Boston University Chobanian & Avedisian School of Medicine, Boston, Massachusetts, USA

[10]Department for Psychiatry and Psychotherapy, University Medical Center of Göttingen, Georg-August University, Göttingen, Germany

[11]Cluster of Excellence "Multiscale Bioimaging: from Molecular Machines to Networks of Excitable Cells" (MBExC), University of Göttingen, Göttingen, Germany

[12]German Center for Cardiovascular Diseases (DZHK), Göttingen, Germany

[13]Center for Computational Biology and Bioinformatics, Indiana University School of Medicine, Indianapolis, Indiana, USA

ACKNOWLEDGMENTS

The authors thank the participants and their families for their time and contributions, and all the ADNI site investigators and team members. The support for this project was provided by the Alzheimer's Disease Neuroimaging Initiative (National Institutes of Health Grant U01 AG024904) and ADNI DOD (Department of Defense award number W81XWH-12-2-0012). Additional support for data analysis was provided by NLM R01 LM012535, NIA R03 AG063250, NIA R01 AG19771, NIA P30 AG10133, NIA P30 AG072976, NIA R01 AG057739, NIA U01 AG024904, NLM R01 LM013463, R01 AG068193, T32 AG071444, U01 AG068057, NIGMS P50GM115318, NCATS UL1 TR001108, NIA K01 AG049050, NIA R01 AG061788, the Alzheimer's Association, the Indiana Clinical and Translational Science Institute, and the IU Health-IU School of Medicine Strategic Neuroscience Research Initiative. Data collection and sharing for this project was funded by the Alzheimer's Disease Neuroimaging Initiative (ADNI) (National Institutes of Health Grant U01 AG024904) and DOD ADNI (Department of Defense award number W81XWH-12-2-0012). ADNI is funded by the National Institute on Aging, the National Institute of Biomedical Imaging and Bioengineering, and through generous contributions from the following: AbbVie; Alzheimer's Association; Alzheimer's Drug Discovery Foundation; Araclon Biotech; BioClinica, Inc.; Biogen; Bristol-Myers Squibb Company; CereSpir, Inc.; Cogstate; Eisai Inc.; Elan Pharmaceuticals, Inc.; Eli Lilly and Company; EuroImmun; F. Hoffmann-La Roche Ltd and its affiliated company Genentech, Inc.; Fujirebio; GE Healthcare; IXICO Ltd.;Janssen Alzheimer Immunotherapy Research & Development, LLC; Johnson & Johnson Pharmaceutical Research & Development LLC; Lumosity; Lundbeck; Merck & Co., Inc.;Meso Scale Diagnostics, LLC; NeuroRx Research; Neurotrack Technologies; Novartis Pharmaceuticals Corporation; Pfizer Inc.; Piramal Imaging; Servier; Takeda Pharmaceutical Company; and Transition Therapeutics. The Canadian Institutes of Health Research is providing funds to support ADNI clinical sites in Canada. Private sector contributions are facilitated by the Foundation for the National Institutes of Health (www.fnih.org). The grantee organization is the Northern California Institute for Research and Education, and the study is coordinated by the Alzheimer's Therapeutic Research Institute at the University of Southern California. ADNI data are disseminated by the Laboratory for Neuro Imaging at the University of Southern California. This research was supported in part by Lilly Endowment, Inc., through its support for the Indiana University Pervasive Technology Institute. This work was supported by NIH RF1AG078299 (I Delalle, JK Blusztajn, A Fischer, A Saykin, K Nho, H Lin, AL DeStefano, A Krunic); NIH U19 AG024904, P30 AG072976 and U19 AG074879 provide funding for A Saykin (also supported by NIH P30 AG010133, R01 AG019771, R01 AG057739, R01 LM013463, R01 AG068193, T32 AG071444, U01 AG068057, U01 AG072177), K Nho (also supported by NIH U01AG072177 and U19 AG074879), S Lui, T Park, Y-N Huang Y-N, and SL Risacher; NIH RF1 AG057768,

P30 AG013846, RF1 AG072654 (JK Blusztajn); NIH U01AG068221 (H Lin and AL DeStefano); NIH U01 AG058589, R01DK122503 (AL DeStefano); The DFG (Deutsche Forschungsgemeinschaft) priority program 1738, SFB1286 and GRK2824;The German Federal Ministry of Science and Education (BMBF) via the ERA-NET Neuron project EPINEURODEVO; The EU Joint Programme- Neurodegenerative Diseases (JPND) – EPI-3E; Germany's Excellence Strategy—EXC 2067/1 390729940 (A Fischer, DM Krueger, T Pena, Pradhan R, S Burkhardt, R Schroeder, N Hempel); GoBIO project miRassay (16LW0055) by the German Federal Ministry of 1 Science and Education (F Sananbenesi, A Schutz). The above funding sources had no role in study design, collection, analysis and interpretation of data, writing of the manuscript, or the decision to submit the article for publication.

CONFLICT OF INTEREST STATEMENT

Dr. Saykin receives support from multiple NIH grants (P30 AG010133, P30 AG072976, R01 AG019771, R01 AG057739, U19 AG024904, R01 LM013463, R01 AG068193, T32 AG071444, U01 AG068057, U01 AG072177, and U19 AG074879). He has also received support from Avid Radiopharmaceuticals, a subsidiary of Eli Lilly (in kind contribution of PET tracer precursor) and participated on scientific advisory boards (Bayer Oncology, Eisai, Novo Nordisk, and Siemens Medical Solutions USA, Inc.) and an observational study monitoring board (MESA, NIH NHLBI), as well as external advisory committees for multiple NIA grants. He also serves as editor-in-chief of *Brain Imaging and Behavior*, a Springer-Nature Journal. Dr. Shannon Risacher served as Communications Chair, unpaid, for the Alzheimer's Association AWARE PIA, as well as received travel funding for the Charleston Conference on Alzheimer's Disease. She also has equity interest in Eli Lilly (< $10000), a company that may potentially benefit in the research results of this study. Dr. Shiwei Liu, Dr. Thea Rosewood, Dr. Kwangsik Nho, Ms. Soumilee Chaudhuri, Ms. Min Young Cho, Dr. Yen-Ning Huang, Dr. Tamina Park have no interests to declare. The funders had no role in the study's design, the collection, analyses, or interpretation of data, the writing of the manuscript, or the decision to publish the results. Author disclosures are available in the supporting information.

CONSENT STATEMENT

All participants provided informed consent.

ORCID

Ivana Delalle https://orcid.org/0000-0002-1873-3064

REFERENCES

1. Atri A. The Alzheimer's disease clinical spectrum: diagnosis and management. *Med Clin North Am*. 2019;103(2):263-293. doi:10.1016/j.mcna.2018.10.009
2. Prince M, Bryce R, Albanese E, Wimo A, Ribeiro W, Ferri CP. The global prevalence of dementia: a systematic review and metaanalysis. *Alzheimers Dement*. 2013;9(1):63-75. doi:10.1016/j.jalz.2012.11.007
3. Scheltens P, Blennow K, Breteler MM, et al. Alzheimer's disease. *Lancet*. 2016;388(10043):505-517. doi:10.1016/S0140-6736(15)01124-1
4. DeTure MA, Dickson DW. The neuropathological diagnosis of Alzheimer's disease. *Mol Neurodegener*. 2019;14(1):32. doi:10.1186/s13024-019-0333-5
5. Jack CR Jr, Bennett DA, Blennow K, et al. A/T/N: an unbiased descriptive classification scheme for Alzheimer disease biomarkers. *Neurology*. 2016;87(5):539-547. doi:10.1212/WNL.0000000000002923
6. Kiko T, Nakagawa K, Tsuduki T, Furukawa K, Arai H, Miyazawa T. MicroRNAs in plasma and cerebrospinal fluid as potential markers for Alzheimer's disease. *J Alzheimers Dis*. 2014;39(2):253-259. doi:10.3233/JAD-130932
7. O'Brien J, Hayder H, Zayed Y, Peng C. Overview of MicroRNA biogenesis, mechanisms of actions, and circulation. *Front Endocrinol (Lausanne)*. 2018;9:402. doi:10.3389/fendo.2018.00402
8. Krol J, Loedige I, Filipowicz W. The widespread regulation of microRNA biogenesis, function and decay. *Nat Rev Genet*. 2010;11(9):597-610. doi:10.1038/nrg2843
9. Huang Y, Shen XJ, Zou Q, Wang SP, Tang SM, Zhang GZ. Biological functions of microRNAs: a review. *J Physiol Biochem*. 2011;67(1):129-139. doi:10.1007/s13105-010-0050-6
10. Saliminejad K, Khorram Khorshid HR, Soleymani Fard S, Ghaffari SH. An overview of microRNAs: biology, functions, therapeutics, and analysis methods. *J Cell Physiol*. 2019;234(5):5451-5465. doi:10.1002/jcp.27486
11. Iacomino G. miRNAs: the road from bench to bedside. *Genes (Basel)*. 2023;14(2):314. doi:10.3390/genes14020314
12. Wang M, Qin L, Tang B. MicroRNAs in Alzheimer's Disease. *Front Genet*. 2019;10:153. doi:10.3389/fgene.2019.00153
13. Cao F, Liu Z, Sun G. Diagnostic value of miR-193a-3p in Alzheimer's disease and miR-193a-3p attenuates amyloid-beta induced neurotoxicity by targeting PTEN. *Exp Gerontol*. 2020;130:110814. doi:10.1016/j.exger.2019.110814
14. Zhang H, Liu W, Ge H, Li K. Aberrant expression of miR-148a-3p in Alzheimer's disease and its protective role against amyloid-beta induced neurotoxicity. *Neurosci Lett*. 2021;756:135953. doi:10.1016/j.neulet.2021.135953
15. Wang R, Zhang J. Clinical significance of miR-433 in the diagnosis of Alzheimer's disease and its effect on Abeta-induced neurotoxicity by regulating JAK2. *Exp Gerontol*. 2020;141:111080. doi:10.1016/j.exger.2020.111080
16. Liu DY, Zhang L. MicroRNA-132 promotes neurons cell apoptosis and activates Tau phosphorylation by targeting GTDC-1 in Alzheimer's disease. *Eur Rev Med Pharmacol Sci*. 2019;23(19):8523-8532. doi:10.26355/eurrev_201910_19166
17. Nagaraj S, Want A, Laskowska-Kaszub K, et al. Candidate Alzheimer's disease biomarker miR-483-5p lowers TAU phosphorylation by direct ERK1/2 Repression. *Int J Mol Sci*. 2021;22(7):3653. doi:10.3390/ijms22073653
18. Zhao H, Feng L, Zhong W, Zhen H, Chi Q, Wang X. Hyperphosphorylation of tau due to the interference of protein phosphatase methylesterase-1 overexpression by MiR-125b-5p in melatonin receptor knockout mice. *Int J Mol Sci*. 2021;22(21):11850. doi:10.3390/ijms222111850
19. Pan K, Chen S, Wang Y, Yao W, Gao X. MicroRNA-23b attenuates tau pathology and inhibits oxidative stress by targeting GnT-III in Alzheimer's disease. *Neuropharmacology*. 2021;196:108671. doi:10.1016/j.neuropharm.2021.108671
20. Kinney JW, Bemiller SM, Murtishaw AS, Leisgang AM, Salazar AM, Lamb BT. Inflammation as a central mechanism in Alzheimer's disease. *Alzheimers Dement (N Y)*. 2018;4:575-590. doi:10.1016/j.trci.2018.06.014
21. Abuelezz NZ, Nasr FE, AbdulKader MA, Bassiouny AR, Zaky A. MicroRNAs as potential orchestrators of Alzheimer's disease-related pathologies: insights on current status and future possibilities. *Front Aging Neurosci*. 2021;13:743573. doi:10.3389/fnagi.2021.743573

22. Ludwig N, Leidinger P, Becker K, et al. Distribution of miRNA expression across human tissues. *Nucleic Acids Res*. 2016;44(8):3865-3877. doi:10.1093/nar/gkw116
23. Diener C, Keller A, Meese E. Emerging concepts of miRNA therapeutics: from cells to clinic. *Trends Genet*. 2022;38(6):613-626. doi:10.1016/j.tig.2022.02.006
24. Kumar S, Reddy PH. MicroRNA-455-3p as a potential biomarker for Alzheimer's disease: an update. *Front Aging Neurosci*. 2018;10:41. doi:10.3389/fnagi.2018.00041
25. Kumar P, Dezso Z, Mackenzie C, et al. P1-234: circulating miRNA biomarkers for Alzheimer's disease. *Alzheimer's Dement*. 2013;9:P238. doi:10.1016/j.jalz.2013.05.458
26. Dong Z, Gu H, Guo Q, et al. Profiling of serum exosome MiRNA reveals the potential of a MiRNA panel as diagnostic biomarker for Alzheimer's disease. *Mol Neurobiol*. 2021;58(7):3084-3094. doi:10.1007/s12035-021-02323-y
27. Cogswell JP, Ward J, Taylor IA, et al. Identification of miRNA changes in Alzheimer's disease brain and CSF yields putative biomarkers and insights into disease pathways. *J Alzheimers Dis*. 2008;14(1):27-41. doi:10.3233/jad-2008-14103
28. Serpente M, Fenoglio C, D'Anca M, et al. MiRNA profiling in plasma neural-derived small extracellular vesicles from patients with Alzheimer's disease. *Cells*. 2020;9(6):1443. doi:10.3390/cells9061443
29. Liu CG, Zhao Y, Lu Y, Wang PC. ABCA1-labeled exosomes in serum contain higher MicroRNA-193b levels in Alzheimer's disease. *Biomed Res Int*. 2021;2021:5450397. doi:10.1155/2021/5450397
30. Liu CG, Song J, Zhang YQ, Wang PC. MicroRNA-193b is a regulator of amyloid precursor protein in the blood and cerebrospinal fluid derived exosomal microRNA-193b is a biomarker of Alzheimer's disease. *Mol Med Rep*. 2014;10(5):2395-2400. doi:10.3892/mmr.2014.2484
31. Nie C, Sun Y, Zhen H, et al. Differential expression of plasma Exo-miRNA in neurodegenerative diseases by next-generation sequencing. *Front Neurosci*. 2020;14:438. doi:10.3389/fnins.2020.00438
32. Weiner MW, Veitch DP, Miller MJ, et al. Increasing participant diversity in AD research: plans for digital screening, blood testing, and a community-engaged approach in the Alzheimer's Disease Neuroimaging Initiative 4. *Alzheimers Dement*. 2023;19(1):307-317. doi:10.1002/alz.12797
33. Nho K, Kueider-Paisley A, MahmoudianDehkordi S, et al. Altered bile acid profile in mild cognitive impairment and Alzheimer's disease: relationship to neuroimaging and CSF biomarkers. *Alzheimers Dement*. 2019;15(2):232-244. doi:10.1016/j.jalz.2018.08.012
34. Schindler SE, Gray JD, Gordon BA, et al. Cerebrospinal fluid biomarkers measured by Elecsys assays compared to amyloid imaging. *Alzheimers Dement*. 2018;14(11):1460-1469. doi:10.1016/j.jalz.2018.01.013
35. Royse SK, Minhas DS, Lopresti BJ, et al. Validation of amyloid PET positivity thresholds in centiloids: a multisite PET study approach. *Alzheimers Res Ther*. 2021;13(1):99. doi:10.1186/s13195-021-00836-1
36. Ebenau JL, Timmers T, Wesselman LMP, et al. ATN classification and clinical progression in subjective cognitive decline: the SCIENCe project. *Neurology*. 2020;95(1):e46-e58. doi:10.1212/WNL.0000000000009724
37. Krüger DM, Pena-Centeno T, Liu S, et al. The plasma miRNAome in ADNI: signatures to aid the detection of at-risk individuals. *Alzheimer's Dement*. 2024;1-16. doi:10.1002/alz.14157
38. Love MI, Huber W, Anders S. Moderated estimation of fold change and dispersion for RNA-seq data with DESeq2. *Genome Biol*. 2014;15(12):550. doi:10.1186/s13059-014-0550-8
39. Huang HY, Lin YC, Cui S, et al. miRTarBase update 2022: an informative resource for experimentally validated miRNA-target interactions. *Nucleic Acids Res*. 2022;50(D1):D222-D230. doi:10.1093/nar/gkab1079
40. Skoufos G, Kakoulidis P, Tastsoglou S, et al. TarBase-v9.0 extends experimentally supported miRNA-gene interactions to cell-types and virally encoded miRNAs. *Nucleic Acids Res*. 2024;52(D1):D304-D310. doi:10.1093/nar/gkad1071
41. Szklarczyk D, Kirsch R, Koutrouli M, et al. The STRING database in 2023: protein-protein association networks and functional enrichment analyses for any sequenced genome of interest. *Nucleic Acids Res*. 2023;51(1):D638-D646. doi:10.1093/nar/gkac1000
42. Data from: Agora AD, Knowledge Portal n.d. (accessed May 26, 2024). doi:10.57718/agora-adknowledgeportal
43. Shannon P, Markiel A, Ozier O, et al. Cytoscape: a software environment for integrated models of biomolecular interaction networks. *Genome Res*. 2003;13(11):2498-2504. doi:10.1101/gr.1239303
44. Zhou Y, Zhou B, Pache L, et al. Metascape provides a biologist-oriented resource for the analysis of systems-level datasets. *Nat Commun*. 2019;10(1):1523. doi:10.1038/s41467-019-09234-6
45. Ritchie ME, Phipson B, Wu D, et al. limma powers differential expression analyses for RNA-sequencing and microarray studies. *Nucleic Acids Res*. 2015;43(7):e47. doi:10.1093/nar/gkv007
46. Urbanowicz R, Zhang R, Cui Y, Suri P. STREAMLINE: a Simple, Transparent, End-To-End Automated Machine Learning Pipeline Facilitating Data Analysis and Algorithm Comparison. In: Trujillo L, Winkler SM, Silva S, Banzhaf W, eds. *Genetic Programming Theory and Practice XIX*. Springer Nature Singapore; 2023:201-231.
47. Mattsson N, Smith R, Strandberg O, et al. Comparing (18)F-AV-1451 with CSF t-tau and p-tau for diagnosis of Alzheimer disease. *Neurology*. 2018;90(5):e388-e395. doi:10.1212/WNL.0000000000004887
48. Samudra N, Lane-Donovan C, VandeVrede L, Boxer AL. Tau pathology in neurodegenerative disease: disease mechanisms and therapeutic avenues. *J Clin Invest*. 2023;133(12):e168553. doi:10.1172/JCI168553
49. Yang TT, Liu CG, Gao SC, Zhang Y, Wang PC. The serum exosome derived MicroRNA-135a, -193b, and -384 were potential Alzheimer's Disease biomarkers. *Biomed Environ Sci*. 2018;31(2):87-96. doi:10.3967/bes2018.011
50. Long JM, Ray B, Lahiri DK. MicroRNA-339-5p down-regulates protein expression of beta-site amyloid precursor protein-cleaving enzyme 1 (BACE1) in human primary brain cultures and is reduced in brain tissue specimens of Alzheimer disease subjects. *J Biol Chem*. 2014;289(8):5184-5198. doi:10.1074/jbc.M113.518241
51. Burgos K, Malenica I, Metpally R, et al. Profiles of extracellular miRNA in cerebrospinal fluid and serum from patients with Alzheimer's and Parkinson's diseases correlate with disease status and features of pathology. *PLoS One*. 2014;9(5):e94839. doi:10.1371/journal.pone.0094839
52. Tan L, Yu JT, Tan MS, et al. Genome-wide serum microRNA expression profiling identifies serum biomarkers for Alzheimer's disease. *J Alzheimers Dis*. 2014;40(4):1017-1027. doi:10.3233/JAD-132144
53. Khoo SK, Petillo D, Kang UJ, et al. Plasma-based circulating MicroRNA biomarkers for Parkinson's disease. *J Parkinsons Dis*. 2012;2(4):321-331. doi:10.3233/JPD-012144
54. Salemi M, Marchese G, Lanza G, et al. Role and dysregulation of miRNA in patients with Parkinson's disease. *Int J Mol Sci*. 2022;24(1):712. doi:10.3390/ijms24010712
55. Schulz J, Takousis P, Wohlers I, et al. Meta-analyses identify differentially expressed micrornas in Parkinson's disease. *Ann Neurol*. 2019;85(6):835-851. doi:10.1002/ana.25490
56. Sibley CR, Seow Y, Curtis H, Weinberg MS, Wood MJ. Silencing of Parkinson's disease-associated genes with artificial mirtron mimics of miR-1224. *Nucleic Acids Res*. 2012;40(19):9863-9875. doi:10.1093/nar/gks712
57. Prodromidou K, Matsas R. Species-Specific miRNAs in human brain development and disease. *Front Cell Neurosci*. 2019;13:559. doi:10.3389/fncel.2019.00559

58. Stevens MT, Saunders BM. Targets and regulation of microRNA-652-3p in homoeostasis and disease. *J Mol Med (Berl)*. 2021;99(6):755-769. doi:10.1007/s00109-021-02060-8
59. Zou AE, Ku J, Honda TK, et al. Transcriptome sequencing uncovers novel long noncoding and small nucleolar RNAs dysregulated in head and neck squamous cell carcinoma. *RNA*. 2015;21(6):1122-1134. doi:10.1261/rna.049262.114
60. He JY, Zhou XQ, Wang WT. Mechanism of miRNA-3679 inhibiting downstream ZADH2-target genes to promote hepatocellular carcinoma cell proliferation. *Sichuan Da Xue Xue Bao Yi Xue Ban*. 2022;53(5):744-751. doi:10.12182/20220960505
61. Ding Q, Markesbery WR, Cecarini V, Keller JN. Decreased RNA, and increased RNA oxidation, in ribosomes from early Alzheimer's disease. *Neurochem Res*. 2006;31(5):705-710. doi:10.1007/s11064-006-9071-5
62. Reza A, Yuan YG. microRNAs Mediated regulation of the ribosomal proteins and its consequences on the global translation of proteins. *Cells*. 2021;10(1):110. doi:10.3390/cells10010110
63. Catalanotto C, Cogoni C, Zardo G. MicroRNA in control of gene expression: an overview of nuclear functions. *Int J Mol Sci*. 2016;17(10):1712. doi:10.3390/ijms17101712
64. Harris R, Miners JS, Allen S, Love S. VEGFR1 and VEGFR2 in Alzheimer's disease. *J Alzheimers Dis*. 2018;61(2):741-752. doi:10.3233/JAD-170745
65. Licht T, Goshen I, Avital A, et al. Reversible modulations of neuronal plasticity by VEGF. *Proc Natl Acad Sci U S A*. 2011;108(12):5081-5086. doi:10.1073/pnas.1007640108
66. Martin L, Bouvet P, Chounlamountri N, et al. VEGF counteracts amyloid-beta-induced synaptic dysfunction. *Cell Rep*. 2021;35(6):109121. doi:10.1016/j.celrep.2021.109121
67. McKhann GM. VEGF links hippocampal activity with neurogenesis, learning, and memory. *Neurosurgery*. 2005;56(1):N8. doi:10.1227/01.neu.0000309498.00494.f7
68. Liu J, Yuan S, Niu X, Kelleher R, Sheridan H. ESR1 dysfunction triggers neuroinflammation as a critical upstream causative factor of the Alzheimer's disease process. *Aging (Albany NY)*. 2022;14(21):8595-8614. doi:10.18632/aging.204359
69. Salzmann A, James S-N, Williams DM, et al. Investigating the relationship between IGF-I, -II and IGFBP-3 concentrations and later-life cognition and brain volume. *J Clin Endocrinol Metab*. 2021;106(6):1617-1629. doi:10.1210/clinem/dgab121
70. Zhang H, Zhang L, Zhou D, Li H, Xu Y. ErbB4 mediates amyloid beta-induced neurotoxicity through JNK/tau pathway activation: implications for Alzheimer's disease. *J Comp Neurol*. 2021;529(15):3497-3512. doi:10.1002/cne.25207
71. Mei L, Nave KA. Neuregulin-ERBB signaling in the nervous system and neuropsychiatric diseases. *Neuron*. 2014;83(1):27-49. doi:10.1016/j.neuron.2014.06.007
72. Luo B, Liu Z, Lin D, et al. ErbB4 promotes inhibitory synapse formation by cell adhesion, independent of its kinase activity. *Transl Psychiatry*. 2021;11(1):361. doi:10.1038/s41398-021-01485-6
73. Abhik Ray C, Kimberly MG, Wyss JM, David M, Marcia NG, Steven LC. Neuregulin-1 and erbB4 immunoreactivity is associated with neuritic plaques in Alzheimer disease brain and in a transgenic model of Alzheimer disease. *J Neuropathol & Experiment Neurol*. 2003;62(1):42-54. doi:10.1093/jnen/62.1.42
74. Kuragano M, Yamashita R, Chikai Y, Kitamura R, Tokuraku K. Three-dimensional real time imaging of amyloid beta aggregation on living cells. *Sci Rep*. 2020;10(1):9742. doi:10.1038/s41598-020-66129-z
75. Tachibana M, Holm ML, Liu CC, et al. APOE4-mediated amyloid-beta pathology depends on its neuronal receptor LRP1. *J Clin Invest*. 2019;129(3):1272-1277. doi:10.1172/JCI124853

SUPPORTING INFORMATION

Additional supporting information can be found online in the Supporting Information section at the end of this article.

How to cite this article: Liu S, Park T, Krüger DM, et al.; for the Alzheimer's Disease Neuroimaging Initiative. Plasma miRNAs across the Alzheimer's disease continuum: Relationship to central biomarkers. *Alzheimer's Dement*. 2024;20:7698–7714. https://doi.org/10.1002/alz.14230